

Aeromagnetic Data Interpretation of Wadi Hawashiya Area for Identifying Surface and Subsurface Structures, North Eastern Desert, Egypt

Hamdy I. E. Hassanein and Khaled S. Soliman*

Faculty of Earth Sciences, KAAU, Jeddah, KSA

**Faculty of Sciences, Cairo University, Egypt*

Received: 20 /1/2008

Accepted: 6 /5/2008

Abstract. The studied area is located within the North Eastern Desert of Egypt. The lithology of this area comprises rocks related to Precambrian, Cambrian, Carboniferous, Albian to Cenomanian, Late Cenomanian to Early Turonian and Quaternary.

Aeromagnetic data are fully analyzed and interpreted where the analysis and interpretation are mainly devoted towards outlining significant surface and subsurface tectonic trends and their relationship with T.C. radiometric anomalous zones.

According to the qualitative interpretation of the geological and aeromagnetic, and its shaded relief maps, the lineament structural map is constructed through the signatures of the contours and shaded relief of the total aeromagnetic data. Werner de-convolution (dyke model) was applied to the aeromagnetic anomaly map. The depth estimates calculated for these major magnetic anomalies range between 0.5 and 3.9 km. lineament structural map and magnetic depth map values have been utilized to construct the interpretation of the main subsurface structures affecting the studied area, which correlate with the previous studies of aeroradiometric anomalous zones all over the study area. The obtained results showed the most significant structural trends affecting the distribution of these radiometric anomalies in the present study area.

Four main tectonic trends are outlined from the total aeromagnetic and shading relief maps. These trends were defined as N60E, N45W and E-W.

Introduction

Wadi Hawashiya area is located in the northern part of the Eastern Desert of Egypt, near the western coast of the Gulf of Suez region, west of Ras Gharib town (Fig.1). The studied area is bounded by latitudes $28^{\circ} 07' 30''$ N and $28^{\circ} 27' 30''$ N, and longitudes $32^{\circ} 20' E$ and $32^{\circ} 50' E$ and approximately 1860 km^2 . Various lithologic associations ranging in age from Precambrian to Quaternary represent the exposed rock units in the study area.

The present study shows the relationships between surface, subsurface structural trending and the distribution of radioactive minerals. Therefore, the aeromagnetic survey aims to investigate the subsurface structural setting. The airborne total-count radiometric survey was used to determine the anomalous radioactive zones in the studied area, which may contain radioactive minerals.

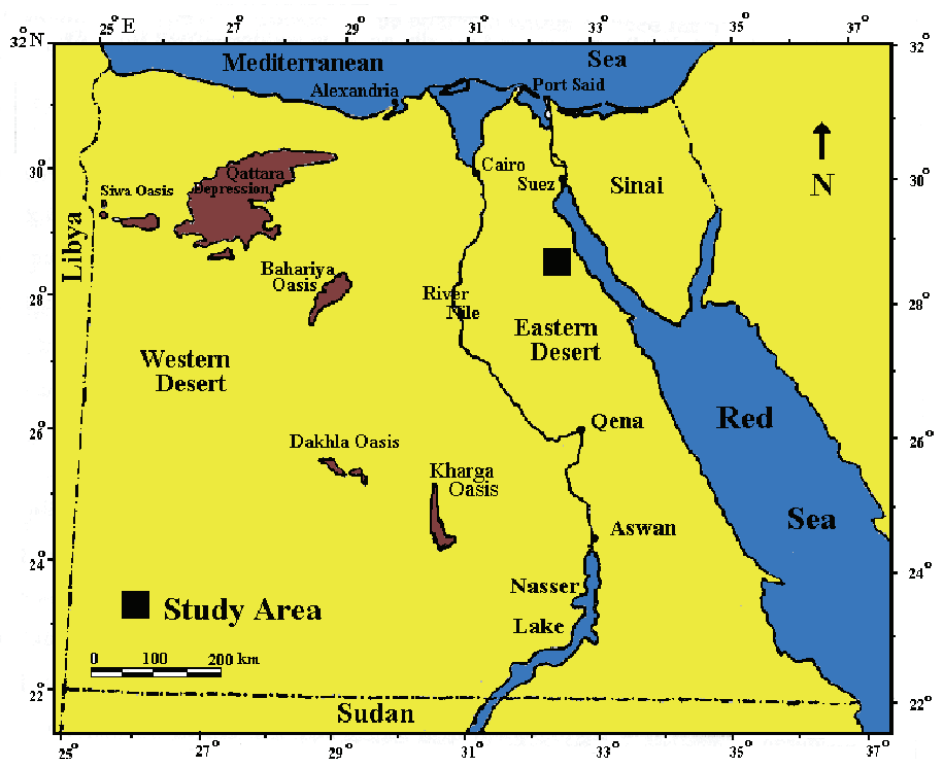


Fig. 1. Map of Egypt showing the location of Gabal Hawashiya North Eastern Desert.

The aeromagnetic survey is a powerful tool in delineating the regional geology (lithology and structure) of buried basement terrain. The detailed aeromagnetic map is proven to be very effective in cases where the geology of the studied area is clearly known (Aero-Service, 1984). According to Reford (1962), the earth magnetic field, acting on magnetic minerals in the crust of the earth induces a secondary field, which reflects the distribution of these minerals. The main field, which is the inducing magnetic field, varies slowly from one place to another.

However, the crustal field, which is the portion of the magnetic field associated with the magnetism of crustal rocks, containing both magnetism caused by induction from the Earth's main magnetic field and from remanent magnetization, varies more rapidly. The airborne magnetometer records these variations in the total magnetic field. The regional correction removes the greater part of the primary field of the earth, so that the local variations of the secondary field are emphasized.

Although several familiar minerals have high susceptibilities (magnetite, ilmenite, and pyrrhotite), magnetite is by far the most common. Rock susceptibility, almost always, is directly related to the percentage of magnetite present. Spatial variations of the crustal field, is usually smaller than the main field, nearly constant in time and place depending on the local geology, where the local magnetic anomalies are the targets in magnetic prospecting. Also, magnetic method is employed, although not always successful, to map topographic features of the basement surface that might influence the structure of overlying sediments. In addition, Large-scale aeromagnetic surveys have been conducted to locate faults, shear zones and fractures. Such zones may serve as potential hosts for a variety of minerals, and may be used as a guidance exploration for the epigenetic, stress-related mineralization in the surrounding rocks (Paterson and Reeves, 1985). The qualitative interpretation of aeromagnetic survey data illustrates directly the geological information by looking at the map without any calculations (Grant and West, 1965). The very high gradient on an aeromagnetic map usually indicates the difference in magnetic susceptibility such as that between granite (acidic rock) andesite (intermediate rock) and basalt (basic rock); a condition called "intra-basement". In case of some variation of contour gradient on an aeromagnetic map, it usually indicates vertical movements (faults); a condition called "supra-basement". The

shape of the causative body also could be considered, in case of circular contours and the magnetization is vertical, where the body may be a plug. In case of elongated closed contours, the source may be a dyke and the direction of elongation should indicate its strike. However, in the case of elongated zone of steep gradient without well-defined closure, it is quite possible that this pattern results from subsurface faulting, which has displaced magnetized rocks (Dobrin, 1976).

Geology

The study area is characterized by a variety of lithological units, where it includes many types of igneous, metamorphic and sedimentary rocks. In addition, the location of the study area at the western side of the Gulf of Suez and in the northern part of the Eastern Desert of Egypt gave the area more important setting. Therefore, there are many different types of works and studies that have been conducted at the studied area.

The study area is represented in sheet No. (NH36SW, Beni Suef, CONOCO, 1987). The geological map of studied area (Fig. 2) delineates that the area is covered by different varieties of basement and sedimentary rock formations. Table 1 shows the stratigraphic succession of the sedimentary and basement rocks, (CONOCO, 1989).

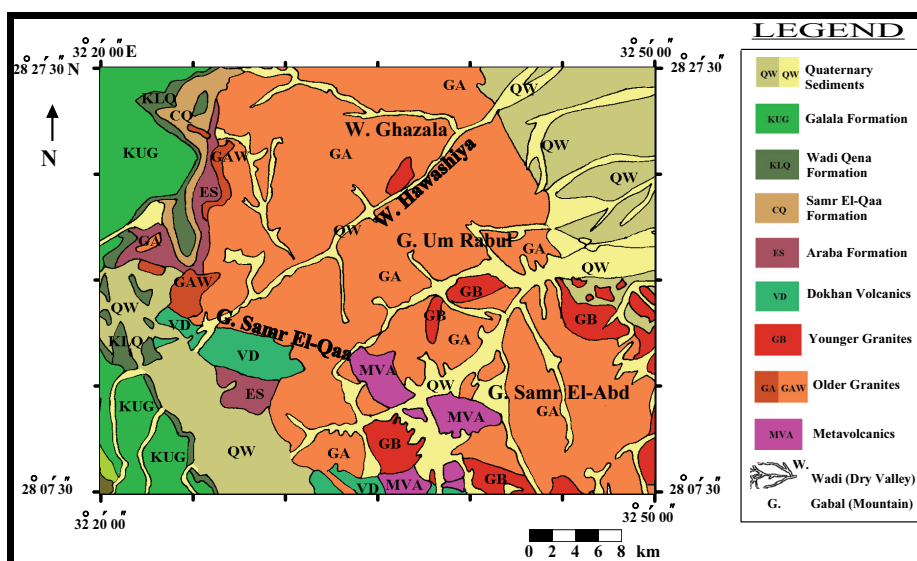


Fig. 2. Geological map, W. Hawashiya area, North Eastern Desert (After Conoco, 1987).

The basement rocks are represented in the eastern part of the studied area as a part of the northern Nubian-Arabian shield at the Egyptian side. These basement rock units mainly are comprised of metavolcanics, Older (Grey) & Younger (Pink) granites. Meanwhile, the western part of the study area is covered by different types of sedimentary rocks that range in age from Paleozoic to Cenozoic. They consist of Cambrian (Araba Formation), Carboniferous (Samr El-Qaa Formation), Albian to Cenomanian (Wadi Qena Formation), Late Cenomanian to Early Turonian (Galala Formation) and Quaternary (Wadi Sediments). The contact zone between the basement and sedimentary successions is considered as an unconformity contact. Kabesh and Abdel-Khalek (1970) gave detailed field and petrographic studies of the late minor intrusive bodies of granitic rocks and their associated dykes in some localities in the northern part of Eastern Desert of Egypt. Nossair (1981 and 1987) studied the southern part of the area under study, where he carried out full petrographical studies on different exposed rock varieties and described the different dyke groups, which intruded the area.

Table 1. The stratigraphic succession of the sedimentary and basement rocks (CONOCO, 1989).

Rock Formation	Lithological composition	Age	Geological setting
Phanerozoic deposits.			
Quaternary Formation(QW)	undifferentiated Sediments	Quaternary	
Galala Formation (KUG)	limestone	Cenomanian-Early Turonian	
Wadi Qena Formation (KLQ)	sandstones	Albian to Cenomanian	
Samr EL-Qaa Formation (CQ)	shale deposits	Carboniferous	
Araba Formation (ES)	sandstones	Cambrian	
Precambrian Basement Rocks			
Younger granites (GB)	the calc- alkaline members [6], ranges from monzo-granite to	Precambrian	more resistant to weathering and occupy terrains of higher relief than the older granite
Older granites (GA)	range in composition from quartz diorites to granodiorites and locally monzonites [6]	Precambrian	Synorogenic, occurs in the form of elongated large bodies parallel to the NW-SE regional structural trend
The intermediate to acidic metavolcanic and metapyroclastics	composed of meta-andesites and metadacites together with subordinate amounts of metabasalts and metarhyolites	Precambrian	They are intimately associated with sediments [6]

Topography- Drainage Pattern

The area of study is dissected by several wadis (dry valleys), which mostly drain to the east in the Gulf of Suez (Fig. 3). It is evident from the distribution of drainage pattern that the trends of the main wadis and their tributaries are structurally controlled. The general outline of the topography of the area under investigation shows that the eastern part of the area is mainly covered by basement complex of relatively high rugged mountains with a number of prominent peaks, mostly formed of volcanic and granitic rocks. Sedimentary rocks mainly cover the western part of the area under study, which is less rugged and less complex than its eastern part. In addition, the area includes a part of Red Sea plain at the east.

Structure

Said (1962) attributed the outcropping of the basement rocks in some localities of the Gulf region to the N-S faulting. He concluded that the tectonic movement in the region is characterized by a double-stress system of both the Aqaba and Suez trends.

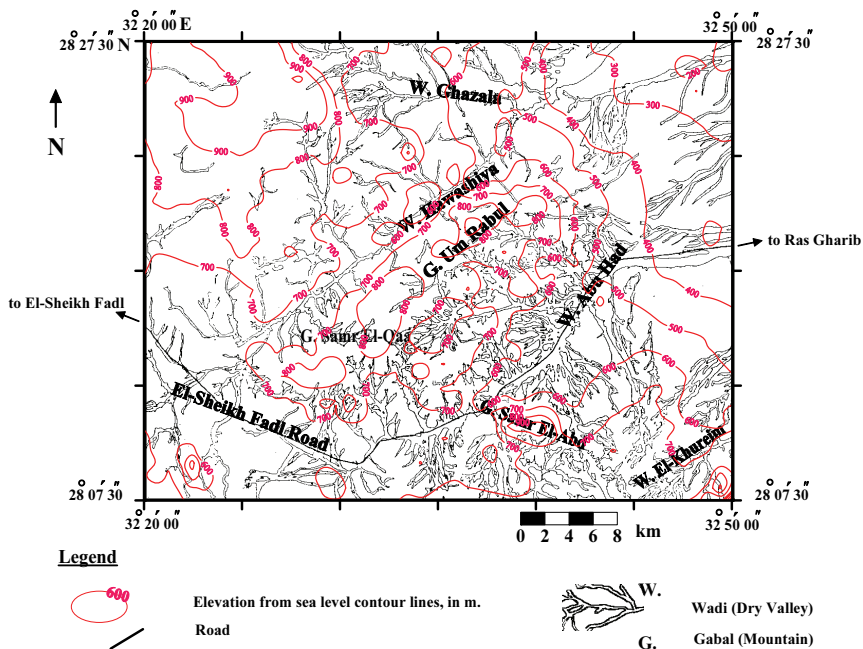


Fig. 3. Topographic drainage of the study area (after military survey department, 1989).

Bayoumi and Boctor (1970) studied the area along the western coast of the Gulf of Suez between latitudes $28^{\circ} 25' N$ and $28^{\circ} 45' N$ and longitudes $32^{\circ} 35' E$ and $33^{\circ} 00' E$, using gravity, magnetic and drill-hole. They concluded that the regional structure of the area, particularly along a NE - SW direction, perpendicular to the general trend pattern of the fault systems, forms major horsts and grabens. In addition, they calculated the average depth to the top of basement complex, where it reached about 3000 meters.

Abdel-Rahman and El-Etr (1980) considered that the NE- and ENE-trends are equally predominating and regionally persisting throughout the entire area of the Eastern Desert. Meshref and El-Sheikh (1973), analyzed the magnetic data obtained over the Gulf of Suez area to define the tectonic trends, which control the structural pattern of the area. The study shows five tectonic trends ($N85^{\circ}E$, $N65^{\circ}E$, $N35^{\circ}E$, $N65^{\circ}W$ and $N35^{\circ}W$). The $N35^{\circ}E$ and the $N35^{\circ}W$ trends are interpreted as a result of the northern compressive force. The $N65^{\circ}W$ trend is interpreted as a result of the local tectonic forces associated with the opening of the Red Sea.

El-Gaby (1983) postulated that the northern part of the Eastern Desert and Southern Sinai of Egypt have been uplifted during the Pan-African Orogeny along a high angle, right lateral thrust- and shear zone. This zone is more than 50 km wide and runs nearly parallel to the Qena-Safaga line, causing the erosion of the Ophiolite thrust sheet and most of the island-arc volcanics, and exposing remobilized rocks of deeper level. Nossair (1981 and 1987) studied the structural setting and detected three major joint sets and three predominant fault trends affecting the various rock exposures in the area: NNE-SSW, NE-SW, NNW-SSE joint sets and NE - SW, N -S, NW-SE fault trends. He also proved that the NE-SW fault trend is the youngest. Figure 4 shows the structure lineaments of the study area (cononco, 1987). The map delineates that the EN-E, NW, N-S and E-W are considered to be the dominant trends recorded in the studied area.

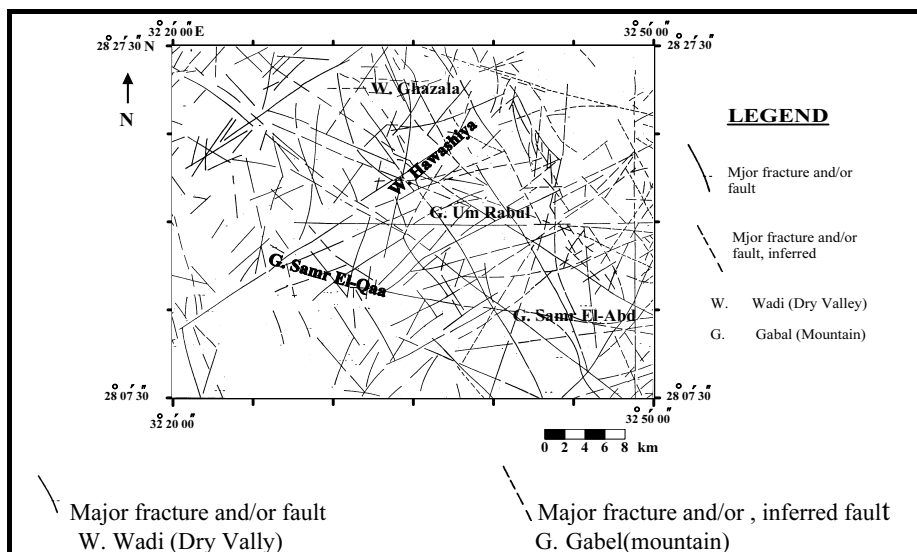


Fig. 4. Detailed structural lineament map of the study area (after Conoco, 1987).

Mineralization

Shalaby (1981) studied the geology and radioactivity of Wadi Khureim, located at the southeastern part of the studied area, and constructed geological and radiometric contour maps on scale 1:40,000, where he analyzed some relatively high radioactive samples. Meshref *et al.* (1992) studied the tectonic framework of the southern part of the Suez rift, using aeromagnetic and Bouguer gravity maps and delineated two different tectonic provinces exist in that area. Regional SW-dipping blocks characterize the southern part, and regional NE-dipping blocks characterize the northern part. An accumulation zone, separating these two accumulation zones, has relatively lower dip angle and relatively shallower depth than the adjacent two blocks. Two types of normal faults may have been developed during the evolution of the faulted blocks. The first-order normal faults were developed during the initial rifting stage and the second-order normal faults were believed to be developed during the major rifting stage. The presence of high tilt angle of the blocks indicates more on and higher magnitude of rifting.

Ammar & others (2003) analyzed the aeroradiospectrometric data to define the radio-spectrometric characters of different lithological units

which are comprised in the area. Accordingly, an interpreted radiometric-lithologic units (IRLU) map is constructed. They defined a number of radiometric anomalous zones. The anomalous zones were considered as probable targets for exploration of radioactive mineralization.

Abdelrahman & others (2007) defined the highly-radioactive zones from the normal radioactive background of the host rocks. The residual T. C. (Fig.5) and the three radioelements (^{40}K , eU & eTh) anomalous zones of the studied area were quantitatively interpreted using least squares method.

Aeromagnetic Survey

The studied area was surveyed using the airborne gamma-ray spectrometric and magnetic, which were conducted by Aero-Service Division, Western Geophysical Company of America in 1984, for the Egyptian General Petroleum Corporation (EGPC) and the Egyptian Geological Survey and Mining Authority (EGSMA). This airborne survey was conducted along most of the Egyptian Eastern Desert.

The aeroradiospectrometric and aeromagnetic surveys were conducted along parallel flight lines oriented in a NE-SW direction at 1.5 km spacing. The total magnetic intensity measurements were carried out using the high-sensitivity (0.01nT) airborne proton free-precision magnetometer (Varian, V-85), mounted in a tail stinger. In addition, the Varian (VIW 2321 G4) single-cell cesium vapour was used as base station magnetometer. The flight lines of the survey were flown along parallel traverse lines in a NE-SW direction, with an azimuth of 45° and 225° from the true north. Meanwhile, the tie lines were flown in a NW-SE direction at right angles to the main flight line direction with an azimuth of 135° and 315° from the true north (Aero-Service, 1984). The traverse flight lines of the studied area were oriented in a northeast-southwest direction at 1.5-kilometre spacing, while the tie lines were flown perpendicularly in a northwest-southeast direction at 10-kilometre intervals. For safety reasons, the flight altitude was 92m in flat terrains and 122m in mountainous terrains (Aero-Service, 1984).

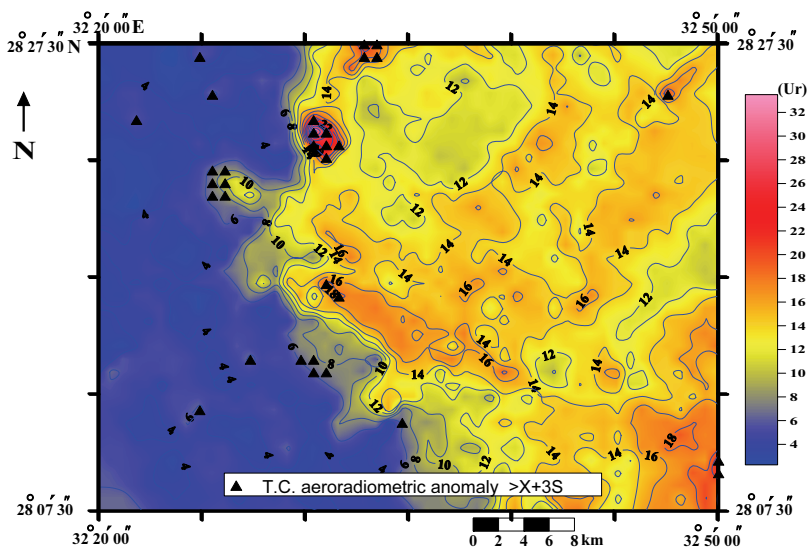


Fig. 5. Total-count (T.C.) aeroradiometric anomaly map (after Abdulrahman, 2007). Aeroradiometric total-count (T.C.) anomaly contour lines, in (Ur).

A crystal-controlled time-of-day clock was synchronized to international time signals using a short-wave radio, so that correlation with the airborne data is assured (Aero-Service, 1984). In addition, a micro-processor based digital recording system using a 9-track, 800-BPI tape system and analog display recorded the total magnetic intensity resolved to 0.01 nano-Tesla (nT) at one second intervals during the periods of flight and generally on a 24-hour basis. The analog recorder was the two-channel Hewlett-Packard (HP-7130A) recorder, consisting of fine (10 nT full-scale) and coarse (100 nT full-scale) output traces, with separate fiducials (Aero-Service, 1984). Diurnal variation effects on the magnetic field, which arise due to solar activities, were recorded using an additional unit of the base station magnetometer (Varian VIW 2321 G4). Also, International Geomagnetic Reference Field (IGRF) is reduced from the total magnetic measurements to get rid of the regional gradient of the earth's magnetic field due to the continual changes in the magnitude and direction of the earth's magnetic field from one place to another (Dobrin, 1976).

The obtained data were corrected and plotted as total aeromagnetic intensity contour maps and profiles. In the this study, the digitizing process follows the basic acquired data analog flight lines drawn on the map and the obtained data are shown as coloured filled contour maps (Fig. 6).

- In sedimentary regions, particularly where the basement depth exceeds 1.5 km, the magnetic contours are normally smooth and variations are small, reflecting the basement rocks rather than the near-surface features (Telford *et al.*, 1990). The magnetic relief observed over sedimentary basin areas is almost always controlled more by the lithology of the basement than by its topography (Dobrin and Savit, 1988). Meanwhile, in regions where igneous and metamorphic rocks predominate, usually exhibit complex magnetic variations. Deep features are frequently camouflaged by higher frequency magnetic effects originating nearer to the surface (Telford *et al.*, 1990).

- Changes in the magnetization of basement rocks a mile or more deep may result in magnetic anomalies up to several thousand gammas(nT) in magnetic readings at the surface. At the same depth, structural relief on the basement surface as great as 900 ft (~ 274.30 m) would seldom produce anomalies larger than 50 gammas (Dobrin and Savit, 1988). The density of contour lines often provides a useful criterion for indicating structures. The closer the contours, *i.e.*, the greater the gradients, the shallower, in general, is the source. Any sudden change in the spacing over an appreciable distance suggests a discontinuity in depth, possibly a fault (Dobrin, 1960).

- The magnetic anomalies of large areal extent reflect a deeper source than small-size anomalies (Vacquier *et al.*, 1951).

- Often, a well-defined boundary between zones with appreciably different degrees of magnetic relief can indicate the presence of a major basement fault (Dobrin and Savit, 1988).

Accordingly, the total-intensity aeromagnetic contour map and shading relief of the total magnetic intensity maps which were constructed (Fig. 7,a,b,c &d) from different horizontal and vertical positioning light angles (HPLA &VPLA), used for outlining the discontinuity lines which dividing the study area into characteristic structural zones. These zones represent the outlines of the local and regional variations in basements structures beneath the study area. Changing of the horizontal positioning light angle (HPLA) helps to define the predominant trends of the subsurface structures in the studied area. Figure 7 shows the NE, NW and approximately E-W are the main trends in the studied area. Figure 8 represents lineament structure map of the studied area using the interpretation of the total magnetic intensity map (Fig. 6) and the different shaded relief map (Fig. 7). Also, figures 5 and 6 show that the total-count anomalous zones are related to the low magnetic zones.

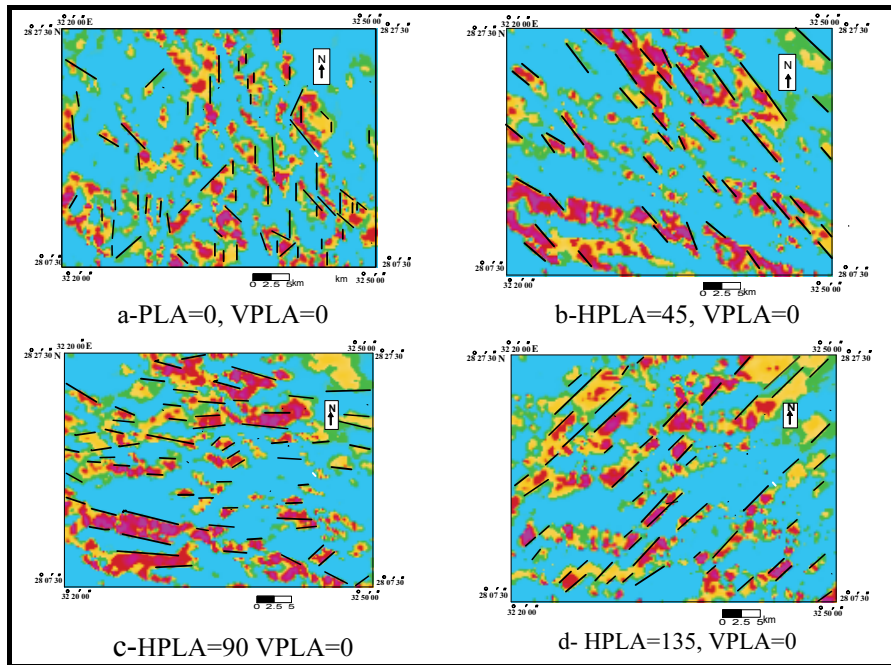


Fig. 7. Shading relief map of total magnetic intensity, to show the main structural trends affecting the study area: a) N-S, b) NW, c) NE and d) E-W trends.
 HPLA= Horizontal positioning light angle. VPLA= Vertical positioning light angle

Quantitative Interpretation

Trend Analysis

Magnetic contours may be drawn out along the fractures, or individual anomalies which may be aligned in relation to fracture system (Hall, 1964). An observed magnetic pattern represented on magnetic contour map is the reflection of the contrast between the magnetic properties of rocks. The observed structural features of the area are reflected significantly in the pattern, where the trends and intensities of magnetic anomalies are shown on the aeromagnetic maps (Danzalski, 1966).

The direction of the various trends of the lineaments along each of the magnetic anomalies (Fig.6), were measured taking into account the azimuth, the length and number of the magnetic trends in each 10 degrees, and presented on a polar plot (by Grapher software, Fig. 9). This figure shows the frequency and length distributions of different trends per 10 degrees azimuth. The azimuth of the long trends defines the

regional trends which control the subsurface structure beneath the studied area. Figure 9 shows that N60° E (Trans African), N45°W (Gulf of Seues), E-W (Mediterranean) trends are the dominant trends effecting the Wadi Hawashiya area. The total count radiometric map (Ammar & others 2003) shows that the distribution of radioactivity in the studied area is mainly controlled by NE & NW trends. Nossier (1981) concluded that the presence of radioactive occurrences is mainly trending in the NE.

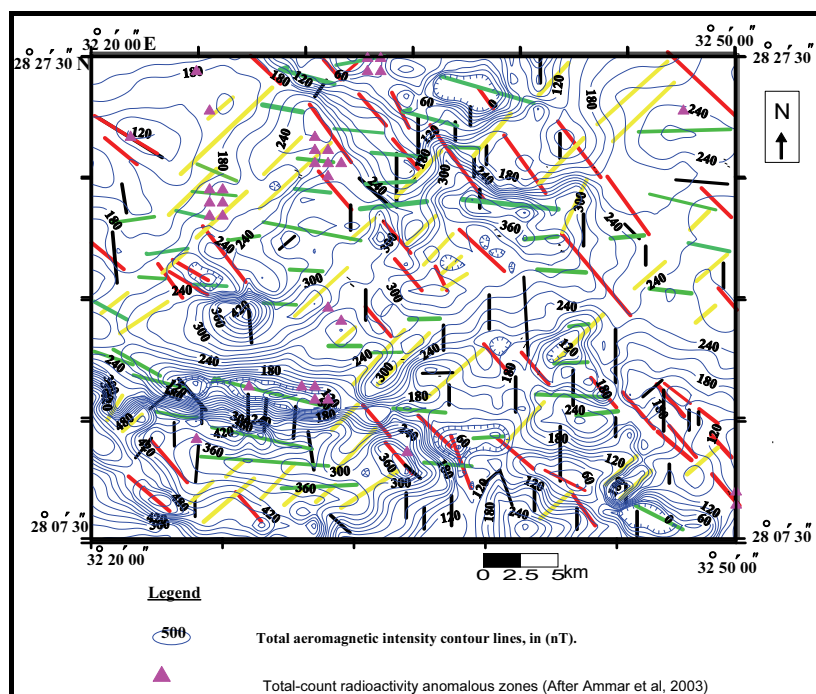


Fig. 8. The interpreted structural lineament map of the study area.

Depth Estimation

The quantitative interpretation of aeromagnetic survey data can be so complex. However, rigorous analysis is carried out on a routine basis only when simple geometrically models are utilized to represent the subsurface sources. In this study, dyke is considered as the predominant structural source of magnetic anomaly. In exploring sedimentary basins, the assumption is generally made that intrusive rocks within the basement are truncated by erosion at their surfaces. If this is the case, the depth to the top of the dyke is equal to the thickness of the sedimentary

section. The intrusives may not be extended upward as the basement surface, therefore, any computed sedimentary thickness is generally considered to be a minimum (Dobrin, 1976).

The depth to the top of the source is a useful tool for finding thickness of sedimentary succession, and sometimes for locating major structures in basement rocks. Some anomalies arise from basement rocks may be due to lithologic changes rather than to structural features. In certain geologic situations, the depth to the bottom of magnetic sources is sought where it can correspond to the Curie-temperature.

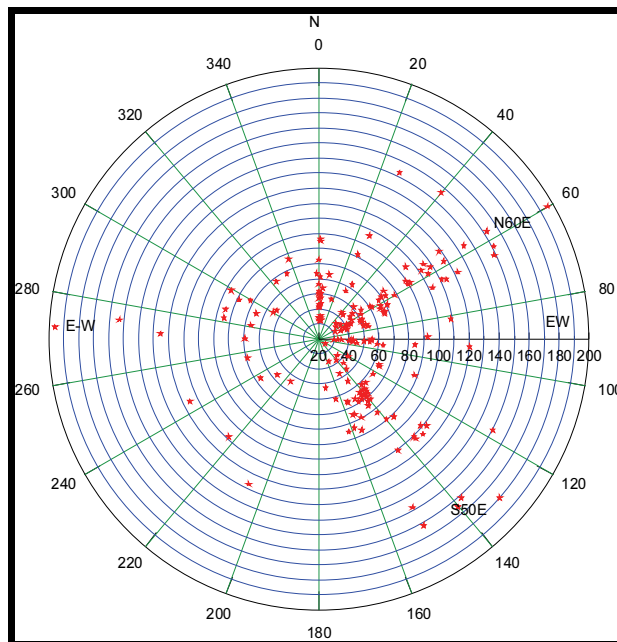


Fig. 9. Polar plot diagram of interpreted structural lineaments of the study area.

The depth to the top surface can be estimated from the form of a magnetic profile, at right angles to the strike, and traversing an anomaly centre or its immediate neighborhood. The strike length can be fairly accurately estimated from the shape of the magnetic anomaly. The depth obtained from a magnetic anomaly is dependent on the selection of appropriate source geometry. Accordingly, the selection of horizontal characteristic parameters can be directly related to the depth of burial (Parasnis, 1966).

In this study, Werner deconvolution is applied on the aeromagnetic data to compute the horizontal and the vertical positions of the magnetic sources, magnetic susceptibility and dip (Werner, 1953). Analysis of the total-intensity magnetic data estimates these parameters where thin sheet-like bodies is considered such as dykes, sills and intruded fault zones. Meanwhile, the analysis of the horizontal gradient, computed from the total-intensity magnetic data, estimates the same parameters for geologic interface features such as dipping contacts, edges of prismatic bodies, major faults, and slope changes of the basement relief. Furthermore, when the horizontal gradient is applied to adequately sensitive data, this technique can identify and resolve very subtle anomalies and yield a significant amount of information (Aero-Service, 1984).

The total magnetic intensity $T(x_i, z, \phi)$ caused by a thin dyke-like structure is given by the equation (Werner, 1953):

$$T(x_i, z, \phi) = k \frac{(x_i - x_0) \sin \phi + z \cos \phi}{(x_i - x_0)^2 + z^2} \quad (1)$$

where:

- k is the amplitude coefficient,
- x_i are discrete points on the ground surface at which $T(x_i, z, \phi)$ is computed,
- x_0 is the location of the thin dyke on the surface,
- z is the depth to the thin dyke, and
- ϕ the index parameter.

Since real data are often influenced by effects of neighboring anomalies or regional fields, interference polynomials can be introduced to compensate for such effects (Werner, 1953 and Hartman *et al.*, 1971). For a first-degree polynomial, equation (1) becomes

$$T(x_i, z, \phi) = k \frac{(x_i - x_0) \sin \phi + z \cos \phi}{(x_i - x_0)^2 + z^2} + A(x_i - x_0) + B \quad (2)$$

where: A and B are constant terms of the first-degree polynomial.

As Ferderer (1988) points out, the interference terms also enable the determination of good parameter estimates over sources that do not satisfy the thin dyke or contact assumption. Solving equation (2) requires

cross multiplying by the denominator and rearranging the expression obtained according to powers of the (x_i), which gives:

$$T^2(x_i) = p_1x_iT - p_2T + p_3x_i^3 + p_4x_i^2 + p_5x_iT + p_6 \quad (3)$$

where:

$$\begin{aligned} p_1 &= x_0, & p_2 &= x_0^2 + z^2, & p_3 &= A, \\ p_4 &= B - 3Ax_0, \\ p_5 &= k \sin \phi + 3Ax_0^2 + Az^2 - 2Bx_0 \quad \text{and} \\ p_6 &= kz \cos \phi + kx_0 \sin \phi + Ax_0^3 - Bx_0^2 - Ax_0z^2 + Bz^2 \end{aligned}$$

Equation (2), which is nonlinear in the unknown parameters (x_0 , z , k , ϕ , A & B), is thus transformed to a form that is linear in the parameters (p_i) in equation (3). Once the (p_i) are determined, the following relations can be used to obtain the unknown magnetic source parameters:

$$\begin{aligned} x_0 &= p_1, & z &= \sqrt{p_2 - p_1^2}, & A &= p_3 \\ B &= p_4 + p_3p_1, & \phi &= \tan^{-1}(k \sin \phi / k \cos \phi) \quad \text{and} \\ k &= (p_5 - 3p_3p_1^2 - p_3(3p_2 - p_1^2) + 2p_1(p_4 - p_3p_1)) / \sin \phi \end{aligned}$$

To determine the p_i , equation (3) is solved using six data points, given a system of six linear equations in six unknowns.

The depth to the top of the intrusive rock ensembles, thin dyke model, is calculated from the aeromagnetic map (Fig. 6) using Werner deconvolution technique (Fig. 10). Figure 10 shows that the computed depths range between 0.5 to 3.9 km. The considerably large depth values are located mainly above the wadis (dry valleys) that cut across the area (e.g., Wadi Hawashiya) and observed their trend at many localities. These relatively large depth values coincide also with the Quaternary sediments. The relatively low depth values are in accordance with the mountainous areas such as G. Samr El-Abd.

These results agree well with both the geologic map (Fig. 2) and the topographic map (Fig. 3) and of the studied area. The depth results obtained helped greatly in interpreting the relief and structure of the buried magnetic basement surface. Figure 10 concluded that the studied area is represented by numerous series of near surface structures (H1, H2, H3, H4, H5, H6, H7, H8, H9, H10, H11, H12, H13 and H14) and deep structures (G1, G2, G3, G4, G5, G6, G7, G8, G9, G10, G11, G12, G13,

G14, G15 and G16). Consequently, Fig. (2, 4, 6 and 10) concluded that: the depth range of near surface basement structures (up-faulted, up-thrown, up-thrusted or raised blocks), beneath the studied area, is 0.5 to 1.6 km. Meanwhile, the deep-seated basement structures (down-faulted, down-thrown, down-thrusted or subsided blocks) are varying in depth between 2.3 to 3.6 km. Step-faulting phenomena are also noticed and evident in many parts of the studied area, especially along the transitional zone between near surface and deep-seated basement structures. These near surface and deep-seated zones cut across and displace each other with different dislocations and different directions. Furthermore; they demonstrate different magnitudes of throws in different directions.

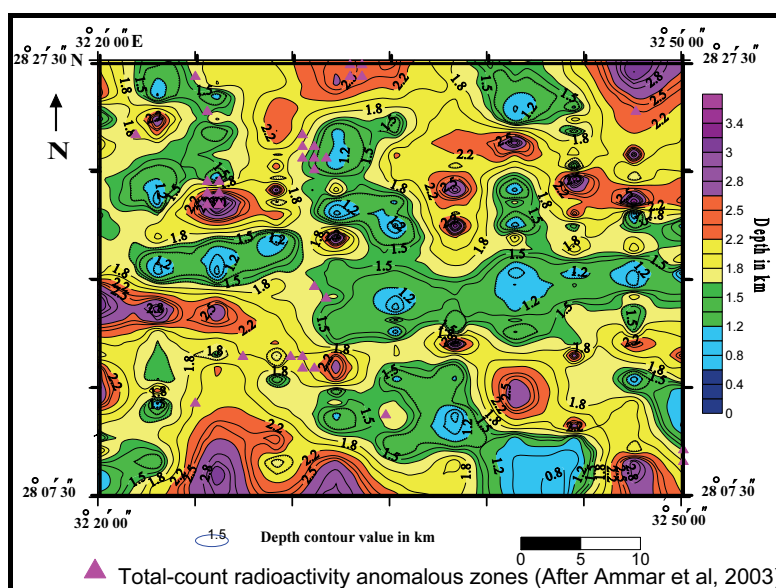


Fig. 10. Interpreted Magnetic depth coloured map as a result of Werner deconvolution technique application on aerial total-magnetic intensity data.

The interpreted depth map shows that the shallow and deep zones are mainly trending ENE, E-W, WE and WNW, affecting the subsurface structures in the studied area. NW-trend mainly cuts across the area and dislocating the ENE, E-W and WNW trending structures.

Discussion and Conclusions

Airborne geophysical study is utilized to delineate the subsurface structure which controls the anomalous mineralization zones of the

studied area. In this study, aeromagnetic magnetic data and the regional geological map are considered as the main sources of information.

According to visual inspection of the various geological and aeromagnetic maps, the subsurface basement tectonic map of studied area is constructed. The depth to the top of the intrusive causative targets, using the thin-dyke model, was calculated from the aeromagnetic map using Werner deconvolution method. It was found that the computed depths range between 0.5 and 3.9 km. The relatively large depth values are observed mainly above the wadis (dry valleys), which cross the area (e.g. Wadi Hawashiya) and observed their trends at many localities. These deep values correspond to the occurrence of the Quaternary sediments. The relatively shallow depth values correspond to the mountainous areas such as: Wadi Hawashiya and G. Samr El-Abd. These results agree well with both topographical and geological maps of the studied area. The interpreted depths helped greatly in the interpretation basement relief. Statistical trend analysis and shading relief magnetic maps helped to delineate N60E, N45W and E-W trends, which are the dominant trends effecting the Wadi Hawashiya area. The total count radiometric map (Ammar *et al.* 2003) shows that the distribution of radioactivity in the studied area is in the trend of NE & NW, which mainly controls the presence of radioactive minerals. The present study delineates that the significant radioactive anomalies lie at the zones which were affected by these two trends, in addition to the E-W trend. Furthermore, the shading relief maps show that the total-count anomalous zones are related to the low magnetic zones which are associated with acidic rocks.

Finally, it could be concluded that, the application of aeromagnetic survey combined with geological studies provide a powerful tool in delineating the lithological and structural setting which may control the mineralization in arid terrains.

Acknowledgements

The authors would like to thank Prof. Dr. Ahmed A. Ammar, professor of applied geophysics, NMA, Exploration Division and Prof. Dr. El-Sayed M. Abdel-Rahman, professor of geophysics, Faculty of Sciences, Cairo University, for their valuable discussions and revising the manuscript.

References

- Ammar, A. A., Abdel-Rahman, M. A., Hassanein, H. I. E. and Soliman, K. S.** (2003) Radiometric lithologic interpretation of aerial radiospectrometric false colour image maps, Eastern Desert, Egypt, *Arab Gulf Journal of Scientific researches*, **21**(1): 28-47.
- Abdel-Rahman, M. A. and El-Etr, H. A.** (1980) The orientational characteristics of the structural grain of the Eastern Desert of Egypt, *In: El-Etr, H. A., Embabi, N. S. and Youssef, M. S. M., (ed.), Geologic-Geomorphic Studies in the Egyptian Deserts*, Ain Shams Uni., Cairo, Egypt, (Abstract), 5 p.
- Abdel-Rahman, M. A., Ammar, A. A., Hassanein, H. I. E. and Soliman, K. S.** (2007) Separation of anomalous aerial radiospectrometric zones using least-squares method on a sample area in Egypt, *The Arabian Journal for Science and Engineering*, **32**, (1A), January 2007.
- Aero-Service** (1984) Final Operational Report of airborne magnetic/ radiation survey in the Eastern Desert, Egypt, Conducted for the Egyptian General Petroleum Corporation, Aero-Service Division, Houston, Western Geophysical Co., Texas, USA.
- Bayoumi, A. I. and Bector, J. G.** (1970) Geological significance of gravity and magnetic anomalies in Rahmi area, Gulf of Suez district, U.A.R. *7th Arab Pet. Con., Secret. Gen. Leag. Arab State, Kuwait, Mar. 1970*, **2** (36): B-2, 28 p.
- Conoco Coral** (1987) *Geological Map of Egypt, Scale 1: 500,000, -NH36SW- Beni Suef, Egypt*. The Egyptian General Petroleum Corporation, Cairo (EGPC), Egypt.
- _____ (1989) *Stratigraphic Lexicon and Explanatory Notes to the Geological Map of Egypt, scale 1:500,000*, Maurice Hermina, Eberhard Klitzsch and Franz K. List., Egypt. 236p.
- Dobrin, M. B.** (1960) *Introduction to Geophysical Prospecting*, McGraw-Hill Book Company, New York, 445p.
- Dobrin, M. B.** (1976) *Introduction to Geophysical Prospecting*, McGraw-Hill Book Company, New York, 630p.
- Dobrin, M. B. and Savit, C. H.** (1988) *Introduction to Geophysical Prospecting*, Fourth Edition, McGraw-Hill Book Company, New York, 867p.
- Danzalski, W.** (1966) Interpretation of aeromagnetic in evaluation of structural control of mineralization, *Geophysics Prosp.*, **14** (3): 273-291.
- El-Gaby, S.** (1983) Architecture of the Egyptian basement complex, *Proceed. 5th Intern. Conf. Basement Tectonics, Cairo, Egypt*.
- Ferderer, R. J.** (1988) Werner deconvolution and its application to the Penokean Oregon, East-Central Minnesota, *Ph.D. Thesis*, Univ. of Minnesota, USA.
- Hartman, R. R., Teskey, D. J. and Friedberg, J. L.** (1971) A system for rapid digital aeromagnetic interpretation, *Geophysics*, **36**: 891-918.
- Hall, D. H.**, (1964) Magnetic and tectonic regionalization on Texada Island, British Columbia, *Geophysics*, **29** (4): 566-308.
- Kabesh, M. L. A., Abdel-khaleak, M. L. and Rafaat, A. M.** (1970) Geology of Wadi El-Mallaha area, Esh El-Mallaha Range, Eastern Desert, U.A.R., *Jour. Geol.*, **4** (2).
- Meshref, W. M. and El-Sheikh, M. M.** (1973) Magnetic tectonic trend analysis in Northern Egypt, *Egypt. Jour. Geol.*, **17**: 179-184.
- Meshref, W. M., Refai, E., Abdel-Hady, Y. E. and Sharaf El-Din, S. M.** (1992) Rift tectonics of the Southern Gulf of Suez: gravity and magnetic contribution, *Proceedings of the Eleventh Petroleum Exploration Conference, the Egyptian General Petroleum Corporation (EGPC), Cairo, Egypt, 7-10 Nov., 1992*, Exploration 1.
- Military Survey Department** (1989) *Topographic Map of Egypt, scale 1: 100, 000, -NH 36, B2-Gabal Samr El-Qaa & -NH 36 .B3- Gabal Gharib, Egypt*, Military Survey Department, Cairo, Egypt.

- Nossair, L. M.** (1981) Relation of radioactivity to fracture system in some basement rocks, North Eastern Desert, Egypt, *M.Sc. Thesis (Unpub.)*, Fac. Sci., Al-Azher University, Egypt.
- Nossair, L. M.** (1987) structural and radiometric studies on Gabal Gharib area, North Eastern Desert, Egypt, *Ph.D. Thesis (Unpub.)*, Fac. Sci., Alexandria University, Egypt.
- Parasnis, D. S.** (1966) *Mining Geophysics*, Elsevier Publishing Co., Amsterdam, London, New York.
- Said, R.** (1962) *The Geology of Egypt*, Elsevier Publ. Co., Amsterdam-New York, 337 p.
- _____ (1971) *The Geological Survey of Egypt*, History and Organization, Geol. Surv. Egypt, Pap. No. 55, 26 p.
- Sharma, P. V.** (1976) *Geophysical Methods in Geology*, Elsevier Scientific Publishing Company, Amsterdam-Oxford-New York, 428 p.
- Telford, W. M., Geldart, L. P. and Sheriff, R. E.** (1990) *Applied Geophysics*, Second Edition, Cambridge University Press.
- Vacquier, V., Steenland, N. C., Henderson, R. G. and Zeitz, I.** (1951) Interpretation of aeromagnetic maps, *Geol. Soc. Am., Memoir*, 47.
- Werner, S.** (1953) *Interpretation of Magnetic Anomalies at Sheet-Like Bodies*, Sverges Geologiska Undersok, Ser. C. C.
- Shalaby, M. H.** (1981) Radioactivity and geology of a pink granite mass in the Red Sea Hills, north Eastern Desert, A. R. E., *M.Sc. Thesis (Unpub.)*, Al-Azher University, Egypt.

تفسير معطيات المسح الجوي المغنطيسي للتعرف على التراكيب تحت السطحية، منطقة وادي حواشية، شمال الصحراء الشرقية، مصر

حمدي إسماعيل السيد حساتين وخالد سليمان سليمان*

قسم الجيوفيزياء - كلية علوم الأرض - جامعة الملك عبدالعزيز -

* قسم الجيوفيزياء - كلية العلوم - جامعة القاهرة

المستخلص. تقع منطقة وادي حواشية المعنية بهذه الدراسة شمال الصحراء الشرقية المصرية، لذا يشتمل التركيب الصخري بهذه المنطقة على صخور ما قبل الكامبري (الدرع العربي-النوبي)، تعلوها صخور عصور الكامبري، و الكربوني، ومابين السينوماني الألبيني والسينوماني المتأخر ومابين التيروني المبكر ثم الرباعي. تعتمد الدراسة الحالية على تحليل وتفسير نتائج معطيات المسح المغنطيسي التي جمعت لمنطقة الدراسة وذلك للتعرف على التراكيب السطحية و تحت السطحية والوجهات التكتونية المؤثرة فيها، وعلاقتها بشادات الإشعاعية الكلية التي سجلت من قبل في الدراسات السابقة.

استطاعت هذه الدراسة من خلال التفسير الكيفي للتغير في شكل وكثافة الخطوط الكنتورية، وخرائط ظل التضاريس التي رسمت من مسقط رأسي يساوي صفر، وأربعة مساقط أفقية مختلفة (صفر، و ٩٠، و ٤٥، و ١٣٥) لتبين الواجهات التركيبية المؤثرة على المنطقة. كما استخدمت طريقة تحليل فرنر في تحديد أعماق الشادات المغنطيسية المحلية، وتمثيلها كخريطة أعماق للتراكيب

المسببة لهذه الشاذات. يتراوح عمق هذه التراكيب بين ٥,٠ و ٩,٣ كم. استخدمت خريطة التخطيط التركيبي في التعرف على الواجهات التكتونية المؤثرة على المنطقة، بمقارنتها بالدراسات السابقة وجد أنها مرتبطة بالشاذات الراديومترية المنتشرة في المنطقة، مما يشير إلى دور هذه الواجهات التكتونية في توزيع العناصر المشعة في المنطقة. هذه الواجهات هي: وجهة شمال ٦٠° شرق، شمال ٤٥° غرب، وشرق - غرب.